

Recent results on magnetic plasma turbulence

Stanislav Boldyrev*, Jean Carlos Perez†, Joanne Mason** and Fausto Cattaneo‡

**Department of Physics, University of Wisconsin-Madison, 1150 University Ave, Madison, WI 53706*

†*Space Science Center & Department of Physics, University of New Hampshire, Durham, NH 03824*

***College of Engineering, Mathematics and Physical Sciences, University of Exeter, EX4 4QF, UK*

‡*Department of Astronomy and Astrophysics, University of Chicago, 5640 S. Ellis Ave, Chicago, IL 60637*

Abstract. Magnetic plasma turbulence is observed over a broad range of scales in the solar wind. We discuss the results of high-resolution numerical simulations of magnetohydrodynamic (MHD) turbulence that models plasma motion at large scales and the results of numerical simulations of kinetic-Alfvén turbulence that models plasma motion at small, sub-proton scales. The simulations, with numerical resolutions up to 2048^3 mesh points in the MHD case and 512^3 points in kinetic-Alfvén case and statistics accumulated over 30 to 150 eddy turnover times, constitute, to the best of our knowledge, the largest statistical sample of steadily driven three dimensional MHD and kinetic-Alfvén turbulence to date.

Keywords: Alfvén waves, Turbulence, Solar Wind

PACS: 52.35.Ra, 95.30.Qd, 96.50.Tf, 96.50.Ci

INTRODUCTION

Magnetic plasma turbulence is observed in the solar wind over a broad range of scales, from scales much larger than the typical plasma scales (ion gyroscale, inertial length) to the sub-proton scales. At large scales, the simplest model for the plasma motion is provided by one-fluid magnetohydrodynamics (MHD) [e.g., 1]. In this case, turbulence can be thought of as consisting of Alfvén modes propagating with the Alfvén velocity along the guide magnetic field and interacting with each other [2]. In the linear case, Alfvén waves have the dispersion relation $\omega = k_z v_A$, where k_z is the wavenumber along the guide field and $v_A = B_0 / \sqrt{4\pi\rho}$ is the Alfvén speed. One of the main properties of Alfvén turbulence is its anisotropic spectral energy transfer [3]. It can be demonstrated numerically, and explained phenomenologically, that the energy gets distributed predominantly over the modes with $k_\perp \gg k_\parallel$, where k_\perp is the wavenumber normal to the guide field. This result is also consistent with the observational data [e.g., 4, 5].

As the small scales are reached, it can be argued that the anisotropic MHD cascade can transform into the cascade of kinetic-Alfvén modes. The argument goes as follows. When the scales comparable to the ion gyroscale (ρ_i) are reached, then, due to the anisotropic energy distribution, we have $\omega \sim k_z v_A \ll k_\perp v_A \sim k_\perp v_{Ti} \sim \Omega_i$, where Ω_i is the ion cyclotron frequency. Therefore, at $k_\perp \sim 1/\rho_i$, the typical frequency of the turbulent fluctuations is smaller than the ion cyclotron frequency, and kinetic-Alfvén modes can be effectively generated. Kinetic Alfvén modes have a different linearized dispersion relation, $\omega \propto k_\perp k_z$, so the character of the turbulence changes qualitatively at sub-proton scales. Phenomeno-

logical dimensional estimates suggest that the energy spectrum of the fluctuations should become steeper [e.g., 6, 7, 8, 9], which is indeed consistent with numerical simulations and observations [e.g., 10, 11, 4, 12, 13].

Due to the faster increase of frequency with the wavenumber, numerical simulations of kinetic-Alfvén turbulence require a significantly smaller time step, and they incur significantly higher computational costs compared to MHD simulations. In this respect, the fluid-like models that we use in our simulations of kinetic-Alfvén turbulence, which are computationally significantly cheaper than their kinetic or gyrokinetic counterparts, allows one to access the inertial intervals and averaging times that are currently unavailable in direct kinetic or gyrokinetic simulations. For comparison, our simulations of kinetic-Alfvén turbulence are performed at the resolution of 512^3 points for tens of dynamical times [9], while the largest gyrokinetic simulations comprise 128^3 mesh points for a few dynamical times [14, 15].

In this contribution we briefly discuss the results of our recent high-resolution numerical simulations of both MHD turbulence and kinetic-Alfvén turbulence. We expect the results to be valuable for the interpretation of solar wind observations and for constraining phenomenological models. For example, the energy spectrum and structures formed in kinetic-Alfvén turbulence are crucial for understanding the mechanism of energy dissipation in turbulence. The questions of whether the dissipation is intermittent or space-distributed and whether the dissipated energy leads to thermalized or accelerated particles depend on the small-scale structure of turbulence. Another recently studied effect, stochastic particle heating by Alfvénic turbulence [16, 17], also depends on the character of turbulence at (sub)proton scales.

MHD TURBULENCE

The incompressible MHD equations take the form

$$\frac{\partial \mathbf{z}^\pm}{\partial t} \mp \mathbf{v}_A \cdot \nabla \mathbf{z}^\pm + (\mathbf{z}^\mp \cdot \nabla) \mathbf{z}^\pm = -\nabla P + \nu \nabla^2 \mathbf{z}^\pm + \mathbf{f}^\pm, \quad (1)$$

where $\mathbf{z}^\pm = \mathbf{v} \pm \mathbf{b}$ are the Elsässer variables, \mathbf{v} is the fluctuating plasma velocity, \mathbf{b} is the fluctuating magnetic field (in units of the Alfvén velocity), $\mathbf{v}_A = \mathbf{B}_0 / \sqrt{4\pi\rho_0}$ is the Alfvén velocity based upon the uniform background magnetic field \mathbf{B}_0 , $P = (p/\rho_0 + b^2/2)$, p is the plasma pressure, ρ_0 is the background plasma density, ν is the fluid viscosity (which, for simplicity, we have taken to be equal to the magnetic diffusivity) and \mathbf{f}^\pm represent forces that drive the turbulence at large scales.

For strong MHD turbulence, Goldreich & Sridhar [3] argued that the pseudo-Alfvén modes are dynamically irrelevant, since due to their polarization they are coupled only to field-parallel gradients, which are small since $k_{\parallel} \ll k_{\perp}$. If one filters out the pseudo-Alfvén modes by setting $\mathbf{z}_{\parallel}^\pm = 0$, it can be shown that the resulting system is equivalent to the Reduced MHD model:

$$\frac{\partial \mathbf{z}^\pm}{\partial t} \mp \mathbf{v}_A \cdot \nabla \mathbf{z}^\pm + (\mathbf{z}^\mp \cdot \nabla_{\perp}) \mathbf{z}^\pm = -\nabla_{\perp} P + \nu \nabla^2 \mathbf{z}^\pm + \mathbf{f}_{\perp}^\pm. \quad (2)$$

Here the fluctuating fields have only two vector components, but each depends on all three spatial coordinates [e.g., 1]. By varying the amplitudes of the external forces, one can drive the turbulence either in the balanced regime ($z^+ \approx z^-$) or in the imbalanced regime ($z^+ \neq z^-$). The latter case is common in nature, and in particular it applies to the solar wind where more Alfvén waves propagate from the sun than toward the sun.

The results of our simulations are presented in Fig. 1 for balanced turbulence, and in Fig. 2 for the imbalanced case. We see that in both cases the spectrum of the total energy $E = 1/2 \int [(z^+)^2 + (z^-)^2]$, as well as the spectra of the individual components $E^+ = 1/2 \int (z^+)^2$ and $E^- = 1/2 \int (z^-)^2$ scale close to $k_{\perp}^{-3/2}$ as the Reynolds number increases. In addition to measuring the spectra of the Elsässer variables, one can measure the Fourier spectra of the magnetic and velocity fluctuations separately. It turns out that they are not identical, at least when the inertial interval cannot be made very large, as in our simulations. Rather, the spectrum of the magnetic field appears to be slightly steeper than the spectrum of the velocity field. This effect is also seen in solar wind measurements [e.g., 18]. The excess of magnetic energy over kinetic energy (the presence of the so-called residual energy) turns out to be a characteristic property of MHD turbulence, e.g. [19, 20, 21].

Another important comment is related to the structure of MHD turbulence. One can measure the so-called

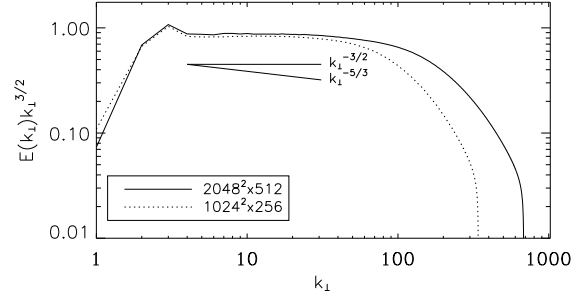


FIGURE 1. Field-perpendicular energy spectra obtained in simulations of magnetohydrodynamic turbulence with a strong guide field.

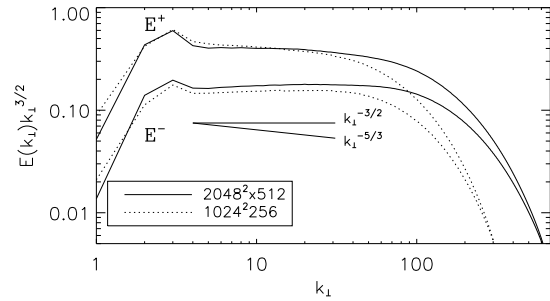


FIGURE 2. Energy spectra $E^+(k_{\perp})$ and $E^-(k_{\perp})$ in imbalanced RMHD as the Reynolds number increases.

scale-dependent dynamic alignment between the magnetic and velocity fluctuations, that is defined as

$$\theta(l) = \langle |\delta \mathbf{v}_{\perp}(\mathbf{l}) \times \delta \mathbf{b}_{\perp}(\mathbf{l})| / \langle |\delta \mathbf{v}_{\perp}(\mathbf{l})| |\delta \mathbf{b}_{\perp}(\mathbf{l})| \rangle, \quad (3)$$

where $\delta \mathbf{v}_{\perp}(\mathbf{l})$ and $\delta \mathbf{b}_{\perp}(\mathbf{l})$ are the field-perpendicular velocity and magnetic field increments, respectively, corresponding to the field-perpendicular scale separation \mathbf{l} . The scaling of the alignment angle can be measured accurately over a broad range of scales, from the inertial interval to the dissipation range, see Fig. 3. The obtained scaling $\theta(l) \propto l^{1/4}$ was proposed to be related to the non-Kolmogorov energy spectrum $k_{\perp}^{-3/2}$; for more discussions see [22, 23, 24].

KINETIC-ALFVÉN TURBULENCE

At scales smaller than the ion gyroscale, turbulence can arguably be dominated by kinetic Alfvén modes. In this case, if the kinetic effects (Landau damping, wave-particle scattering) can be neglected, the dynamics of the magnetic field fluctuations (expressed through the magnetic potential component A_z) and the electron density

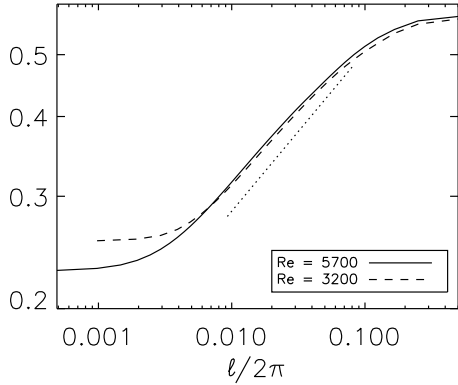


FIGURE 3. Measurements of the dynamic alignment angle (3) in balanced RMHD. The dotted line has a slope of $1/4$. The largest simulations have a resolution of 2048^3 .

fluctuations (n_e) can be described by the so-called two-field system [e.g., 25, 26, 27, 9]. Using the normalized electron density n , and the normalized magnetic potential ψ , we have

$$\partial_t \psi + \nabla_{\parallel} n = \eta \nabla_{\perp}^2 \psi + f_{\psi}, \quad (4)$$

$$\partial_t n - \nabla_{\parallel} \nabla_{\perp}^2 \psi = \nu \nabla_{\perp}^2 n + f_n. \quad (5)$$

whith the normalization: $n = (1 + T_i/T_e)^{1/2} (v_s/v_A) n_e/n_0$ and $\psi = (v_s/c) e A_z / T_e$, where $v_s = (T_e/m_i)^{1/2}$ is the ion-acoustic speed. In addition, the spatial scales are normalized to the ion-acoustic scale ρ_s , and the time scale to $(\rho_s/v_A)(1 + T_i/T_e)^{-1/2}$.¹ The large-scale forces supply energy at large scales, while the small dissipation terms serve to remove the energy at small scales (and they are mostly needed to stabilize the code).

The nonlinearity enters this system through the operator ∇_{\parallel} , which denotes the derivative along the magnetic field that has both mean and fluctuating parts, that is, $\nabla_{\parallel} = \nabla_z + \hat{z} \times \nabla \psi \cdot \nabla_{\perp}$. The nonlinearity thus comes through magnetic line bending due to magnetic fluctuations. In the linear case, which is obtained by replacing $\nabla_{\parallel} \rightarrow \nabla_z$, we obtain the dispersion relation for the kinetic-Alfvén waves $\omega = k_z k_{\perp}$. In these waves, magnetic fluctuations are in equipartition with the density fluctuations, that is, $n_k = \pm |\mathbf{k}_{\perp}| \psi_k$.

Without the forcing and the dissipation terms the system (4, 5) conserves the total energy, E , and the cross-correlation, H ,

$$E = \int (|\nabla_{\perp} \psi|^2 + n^2) d^3x, \quad H = \int \psi n d^3x. \quad (6)$$

¹ Here we present the results derived for small plasma beta. As discussed in [27, 9], essentially the same dimensionless model applies for $\beta \sim 1$ as well.

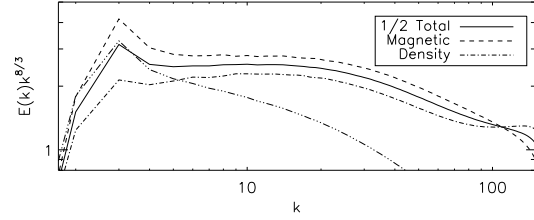


FIGURE 4. Energy spectrum of strong kinetic-Alfvén turbulence at sub-proton scales, obtained in two-field numerical simulations of [9]. For comparison, the dash-triple-dot line shows the total spectrum compensated by $k^{7/3}$.

In a turbulent state, the energy cascades toward small scales while the cross-correlation cascades toward large scales. The energy spectrum produced in the numerical simulations is shown in Fig. 4. The measured spectrum is close to $-8/3$, which is steeper than the $-7/3$ predicted by phenomenological theories based on dimensional arguments [e.g., 6, 7]. It is interesting that a spectrum closer to $-8/3$ was also recently inferred from observations of subproton magnetic and density fluctuations in the solar wind [e.g., 4, 11, 12].

We note that the magnetic energy exceeds the kinetic energy at all scales in the inertial interval. Our simulations (not shown here) demonstrate that this effect is not related to the forcing routine; the excess of magnetic energy in the inertial interval is also observed in simulations where only the density field is forced or where both the density and magnetic fields are forced at large scales. This effect is analogous to the generation of residual energy in MHD turbulence, where the magnetic energy also provides the dominant contribution. We also point out that it is the total energy rather than its density and magnetic-field related components that has a good scaling, in close analogy with MHD turbulence.

Various explanations have been proposed for the steeper than $-7/3$ spectrum of subproton turbulence observed in the solar wind. They include steepening of the spectrum by Landau damping, weakening of turbulence, wave-particle interactions, etc. [e.g., 28, 29]. In our model wave-particle interactions are absent, however, the steeper spectrum persists. A possible explanation proposed in [9] invoked intermittency corrections that result from two-dimensional structures formed by density and magnetic fluctuations. They point to an interesting possibility that the observed scaling is not an artifact of non-universal or dissipative effects, rather, it is an inherent property of the nonlinear turbulent dynamics. The spectrum may therefore be universal, analogous to the Kolmogorov spectrum of fluid turbulence. A definitive numerical study that requires higher numerical resolution will be conducted in due course.

ACKNOWLEDGMENTS

This work was supported by the NSF/DoE partnership grant NSF-ATM-1003451 at the University of New Hampshire, the NSF sponsored Center for Magnetic Self-Organization in Laboratory and Astrophysical Plasmas at the University of Chicago and the University of Wisconsin - Madison, the US DoE awards DE-FG02-07ER54932, DE-SC0003888, DE-SC0001794, the NSF grants PHY-0903872 and AGS-1003451, and the DoE INCITE 2010 Award. This research used resources of the Argonne Leadership Computing Facility at Argonne National Laboratory, supported by the DoE Office of Science under contract DE-AC02-06CH11357. The studies were also supported by advanced computing resources provided by the NSF XSEDE allocation TG-PHY110016 at the National Institute for Computational Sciences and the PADS resource (NSF grant OCI-0821678) at the Computation Institute, a joint institute of Argonne National Laboratory and the University of Chicago.

REFERENCES

1. Biskamp, D., *Magnetohydrodynamic Turbulence*. (Cambridge University Press, Cambridge 2003).
2. Kraichnan, R. H., Inertial-range spectrum of hydromagnetic turbulence, *Phys. Fluids*, **8** (1965) 1385.
3. Goldreich, P. & Sridhar, S., Toward a theory of interstellar turbulence. 2: Strong Alfvénic turbulence, *Astrophys. J.* **438** (1995) 763.
4. Chen, C. H. K., Horbury, T. S., Schekochihin, A. A., Wicks, R. T., Alexandrova, O., & Mitchell, J., Anisotropy of Solar Wind Turbulence between Ion and Electron Scales, *Physical Review Letters*, 104 (2010) 255002.
5. Wicks, R. T., Horbury, T. S., Chen, C. H. K., & Schekochihin, A. A., Anisotropy of Imbalanced Alfvénic Turbulence in Fast Solar Wind, *Physical Review Letters*, 106 (2011) 045001.
6. Biskamp, D., Schwarz, E., Zeiler, A., Celani, A., & Drake, J. F., Electron magnetohydrodynamic turbulence, *Physics of Plasmas*, 6 (1999) 751.
7. Cho, J. & Lazarian, A., Simulations of Electron Magnetohydrodynamic Turbulence, *Astrophys. J.*, 701 (2009) 236.
8. Dastgeer, S. & Zank, G. P., Anisotropic Turbulence in Two-dimensional Electron Magnetohydrodynamics, *Astrophys. J.*, 599 (2003) 715.
9. Boldyrev, S. & Perez, J. C., Spectrum of kinetic-Alfvén turbulence, *Astrophys. J. Lett*, 758 (2012) L44.
10. Sahaoui, F., Goldstein, M. L., Robert, P., & Khotyaintsev, Y. V., Evidence of a Cascade and Dissipation of Solar-Wind Turbulence at the Electron Gyroscale, *Physical Review Letters*, 102 (2009) 231102.
11. Alexandrova, O., Lacombe, C., Mangeney, A., & Grappin, R., Fluid-like dissipation of magnetic turbulence at electron scales in the solar wind, *ArXiv e-prints:1111.5649* (2011).
12. Chen, C. H. K., Salem, C. S., Bonnell, J. W., Mozer, F. S., & Bale, S. D., Density Fluctuation Spectrum of Solar Wind Turbulence between Ion and Electron Scales, *Physical Review Letters*, 109 (2012) 035001
13. Salem, C. S., Howes, G. G., Sundkvist, D., Bale, S. D., Chaston, C. C., Chen, C. H. K., & Mozer, F. S., Identification of Kinetic Alfvén Wave Turbulence in the Solar Wind, *Astrophys. J.*, 745 (2012) L9.
14. Howes, G. G., Dorland, W., Cowley, S. C., Hammett, G. W., Quataert, E., Schekochihin, A. A., & Tatsuno, T., Kinetic Simulations of Magnetized Turbulence in Astrophysical Plasmas, *Physical Review Letters*, 100 (2008) 065004
15. TenBarge, J. M. & Howes, G. G., Evidence of critical balance in kinetic Alfvén wave turbulence simulations, *Physics of Plasmas*, 19 (2012) 055901.
16. Chandran, B. D. G., Li, B., Rogers, B. N., Quataert, E., & Germaschewski, K., Perpendicular Ion Heating by Low-frequency Alfvén-wave Turbulence in the Solar Wind, *Astrophys. J.*, 720 (2010) 503.
17. Xia, Q.; Chandran, B. D.; Perez, J. C.; Cicart, Perpendicular Ion Heating in Low-frequency Alfvén-wave Turbulence, *American Geophysical Union, Fall meeting 2011*, abstract SH43C-1974.
18. Boldyrev, S., Perez, J.-C., Borovsky, J., and Podesta, J., Spectral scaling laws in MHD turbulence simulations and in the solar wind, *Astrophys. J. Letters*, 741 (2011) L19.
19. Boldyrev, S. & Perez J.-C., Spectrum of Weak Magnetohydrodynamic Turbulence, *Phys. Rev. Lett.* **103** (2009) 225001.
20. Wang, Y., Boldyrev, S., & Perez, J.-C., Residual Energy in Magnetohydrodynamic Turbulence, *Astrophys. J. Letters* **740** (2011) L36.
21. Boldyrev, S., Perez, J.-C. & Zhdankin, V., Residual energy in magnetohydrodynamic turbulence and in the solar wind, (2011) eprint arXiv:1108.6072.
22. Boldyrev, S., Spectrum of MHD turbulence, *Phys. Rev. Lett.* **96** (2006) 115002.
23. Mason, J., Cattaneo, F., & Boldyrev, S., Numerical measurements of the spectrum in magnetohydrodynamic turbulence, *Physical Review E*, 77 (2008) 036403
24. Perez, J.-C., Mason, J., Boldyrev, S. & Cattaneo, F., On the energy spectrum of strong MHD turbulence, *Physical Review X*, to appear (2012), eprint arxiv:1209.2011
25. Camargo, S. J., Scott, B. D., & Biskamp, D., The influence of magnetic fluctuations on collisional drift-wave turbulence, *Physics of Plasmas*, 3 (1996) 3912.
26. Terry, P. W., McKay, C., & Fernandez, E., The role of electron density in magnetic turbulence, *Physics of Plasmas*, 8 (2001) 2707.
27. Schekochihin, A. A., Cowley, S. C., Dorland, W., Hammett, G. W., Howes, G. G., Quataert, E., & Tatsuno, T., Astrophysical Gyrokinetics: Kinetic and Fluid Turbulent Cascades in Magnetized Weakly Collisional Plasmas, *Astrophys. J. Supp.*, 182 (2009) 310.
28. Rudakov, L., Mithaiwala, M., Ganguli, G., & Crabtree, C., Linear and nonlinear Landau resonance of kinetic Alfvén waves: Consequences for electron distribution and wave spectrum in the solar wind, *Physics of Plasmas*, 18 (2011) 012307.
29. Howes, G. G., Tenbarge, J. M., & Dorland, W., A weakened cascade model for turbulence in astrophysical plasmas, *Physics of Plasmas*, 18 (2011) 102305.